ChemComm

Mechanistic Insight into Rapid Oxygen-Atom Transfer from a Calix-Functionalized Polyoxovanadate

Journal:	*ChemComm*
Manuscript ID	CC-COM-02-2022-001228.R1
Article Type:	Communication

COMMUNICATION

Mechanistic Insight into Rapid Oxygen-Atom Transfer from a Calix-Functionalized Polyoxovanadate

Received 00th January 20xx,
Accepted 00th January 20xx

DOI: 10.1039/x0xx00000x

Alex. A. Fertig,[a] Shannon E. Cooney,[a] Rachel L. Meyer,[a] William W. Brennessel,[a] and Ellen M. Matson*[a]

We report accelerated rates of oxygen-atom transfer from a polyoxovanadate-alkoxide cluster following functionalization with a 4-tertbutylcalix[4]arene ligand. Incorporation of this electron withdrawing ligand modifies the electronics of the metal oxide core, favoring a mechanism in which the rate of oxygen-atom transfer is limited by outer-sphere electron transfer.

Oxygen-atom transfer (OAT) is an important reaction in industrially relevant processes of relevance to the production of energy-dense chemical fuels.[1, 2] Reducible metal oxides are used prominently as catalysts, and have been shown to facilitate the transfer of O-atoms through the Mars-van Kreveln mechanism.[1, 3] Following formation of a surface O-atom defect site, the resultant coordinatively unsaturated, reduced metal ion is capable of facilitating small molecule activation via OAT. Given the importance of material surfaces for the mediation of these chemical transformations, scientists have invoked the use of nanocrystalline variants.[4] These systems are ideal, as they have a large surface to volume ratio allowing for a maximum number of active sites in the system. Despite the fact that surface bound ligands are commonly employed in order to control solubility of these nanoscopic assemblies,[5] there have been limited studies analysing the physicochemical impact of organosubstitution of the metal oxide core on the resultant reactivity of the system.

Despite advances in sample preparation and spectroscopic techniques, direct analyses into the structure-function relationships that dictate the formation of O-atom defect sites at metal oxide surfaces remain rare. Inspired by this, researchers have turned to the use of atomically precise, redox active metal oxide assemblies, known as polyoxometalates (POMs), as analogues for their bulk congeners.[6-9] POMs are composed of redox-active transition metal oxyanions, linked together in discreet, three-dimensional architectures. Our group has been studying a subset of these molecular assemblies, known as polyoxovanadate-alkoxide (POV-alkoxide) clusters. These vanadate ions are unique in that all bridging oxido positions are saturated by alkoxide moieties, isolating reactivity to terminal V=O groups.[10-12] Notably, we have demonstrated the formation of defect sites at the surface of POV-alkoxides through the transfer of O-atoms.[6, 9, 13] This reactivity is of particular interest, as *in situ* spectroscopic methods allow for detailed kinetic and mechanistic analysis of these reactions,[14] providing insight into O-atom vacancy formation at the surface of metal oxide materials.

Aiming to elucidate the impact ligands have on defect formation at metal oxide surfaces, we extended our initial work exploring OAT between vanadium oxide clusters and phosphanes to a POV-alkoxide bearing *heteroleptic* ligand substitution patterns (Figure 1).[15] In particular, we became interested in studying the reactivity of a POV-alkoxide functionalized with a calix ligand (calix = 4-tert-butylcalix[4]arene), as these clusters have been demonstrated to possess electronic structures influenced by the polydentate ligand.[16] To access the calix-functionalized analogue to the $[V_6O_7(OR)_{12}]$ cluster, oxidation of the previously reported assembly, $[(calix)V_6O_6(OCH_3)_8L]$ (**1**, L = MeCN; structural characterization obtained by single crystal X-ray diffraction, see Figure S1, Tables S1-S2), with iodosyl benzene was performed (Scheme 1). Following work-up, the product,

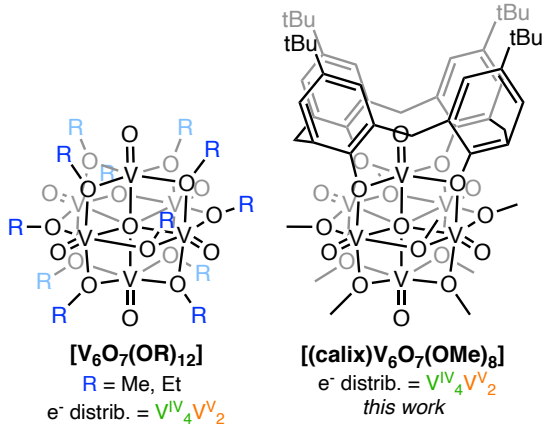

Figure 1. Polyoxovanadate-alkoxide clusters studied in this work.

[a] *Department of Chemistry, University of Rochester, Rochester NY 14627 USA*
Electronic Supplementary Information (ESI) available: Synthetic and other experimental procedures, spectroscopic data, general crystallographic information. CCDC 2145266 (**1**), 2145268 (**2**) and 2145267 (**2-OPMe$_2$Ph**). For ESI and crystallographic data in CIF format see DOI: 10.1039/x0xx00000x

Scheme 1. Synthesis of [(calix)$V_6O_7(OCH_3)_8$] (**2**) and [(calix)$V_6O_6(OPMePh_2)(OCH_3)_8$] (**2-OPMe$_2$Ph**).

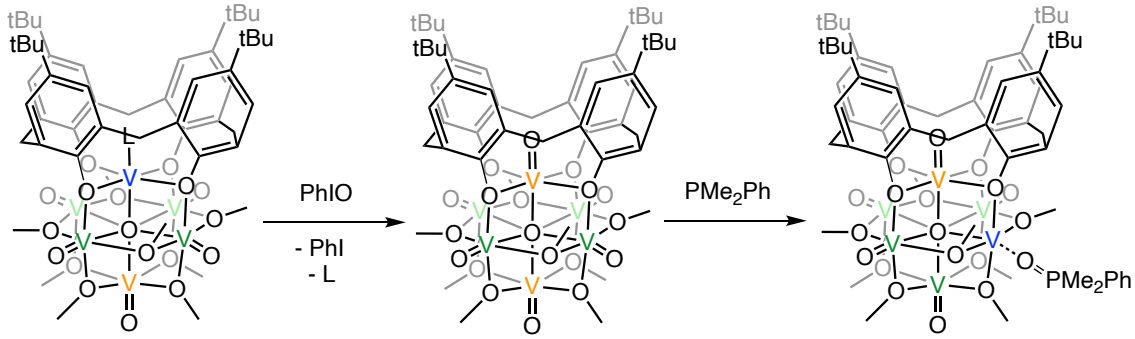

[(calix)$V_6O_6(OMe)_8(MeCN)$]
1 (L = MeCN)
e$^-$ distrib: $V^{III}V^{IV}_4V^{V}_2$

[(calix)$V_6O_7(OMe)_8$]
2
e$^-$ distrib: $V^{IV}_4V^{V}_2$

[(calix)$V_6O_6(OPMe_2Ph)(OMe)_8$]
2-OPMe$_2$Ph
e$^-$ distrib: $V^{III}V^{IV}_4V^{V}$

[(calix)$V_6O_7(OCH_3)_8$] (**2**) was isolated as a green-brown solid in quantitative yield.

To unambiguously confirm the formation of **2**, crystals suitable for single crystal X-ray diffraction were grown from a concentrated acetonitrile solution (Figure 2; see Table S1 for complete crystallographic and refinement parameters). Refinement of the data revealed the expected structure. Each chemically distinct vanadium centre within the cluster core was refined in a crystallographically unique position, allowing for bond valence sum calculations to be employed to verify the oxidation state distribution of the assembly (Table S3).[17, 18] The site differentiated vanadium positioned at the centre of the calix ligand is found to be in a pentavalent oxidation state. The V(V) centre is oxidized by two electrons from that of **1**, consistent with the transfer of an oxygen atom from iodosyl benzene to the calix-bound V(III) centre of the starting material (see Tables S2-S3). The remaining vanadyl ions of the Lindqvist core possess identical oxidation state distributions in complexes **1** and **2**; the vanadyl ion located directly across the cluster core was determined to be a vanadium(V) centre in both compounds. All four vanadium ions in the equatorial plane are best described as V(IV), resulting in an overall oxidation state distribution of for **2** of $V^{IV}_4V^{V}_2$. This assignment of formal oxidation states for complex **2** resembles that reported for the neutral POV-alkoxide cluster, [$V_6O_7(OR_{12})$] (R = CH_3, C_2H_5).[19, 20]

We next explored the OAT reactivity of **2** with a phosphane. Addition of four equivalents of dimethylphenhylphosphine (PMe_2Ph) to **2** resulted in an immediate colour change to brown. The product, [(calix)$V_6O_6(OMe)_8(OPMe_2Ph)$] (**2-OPMe$_2$Ph,**) was isolated as a brown solid (42%, Scheme 1). Evidence for successful V=O bond activation was noted in the IR spectrum of **2-OPMe$_2$Ph**; a transition observed at 1157 cm^{-1} is assigned to ν(O=P) of a datively bound phosphine oxide moiety, indicating OAT from the cluster to PMe_2Ph (Figure S2, Table S3). A similar feature has been reported for [$V_6O_6(OR)_{12}(OPMe_2Ph)$] (R = Me, 1159 cm^{-1}; R = Et, 1157 cm^{-1}).[15] The IR spectrum of **2-OPMe$_2$Ph** also possesses transitions at 1045 and 987 cm^{-1}, corresponding to the ν(O_b-Me) and ν(V=O_t) vibrations of the Lindqvist assembly, respectively. The separation of these two features ($\Delta\nu$ = 58 cm^{-1}) is greater than that of complex **2** ($\Delta\nu$ = 44 cm^{-1}), consistent with reduction the cluster core upon OAT.[15] Reduction of the cluster is further supported through analysis of its electronic absorption spectrum (Figure S3); loss of the $V^{IV}(d_{xy}) \rightarrow V^{V}(d_{x2-y2})$ IVCT at 390 nm observed in **2** (4270 M^{-1} cm^{-1}) and a decrease in the intensity of the $V^{IV}(d_{xy}) \rightarrow V^{V}(d_{xy})$ IVCT at ~1000 nm (460 M^{-1} cm^{-1}) were observed, consistent with reduction of a vanadium(V) centre in the Lindqvist core to vanadium(III) upon OAT.[13]

The ^{1}H NMR spectrum of the purified product revealed the bridging methoxide proton signals have split into five resonances (Figures S4-S5), consistent with a C_S symmetric molecule. This observation suggests activation of a V=O bond positioned *cis* to the calix-functionalized vanadium centre. To unambiguously confirm the site of V=O bond activation, crystals suitable for structural analysis via single crystal X-ray diffraction were grown from slow diffusion of diethyl ether into a concentrated acetonitrile solution (Figure 2, see table S1 for complete crystallographic and refinement parameters). Indeed, formation of the expected product, **2-OPMe$_2$Ph**, with the $OPMe_2Ph$ moiety located in the *cis* position was observed. Disorder between the [$VOPMe_2Ph$] unit and its neighbouring vanadyl moiety prevented bond metric analysis of the equatorial vanadium ions.

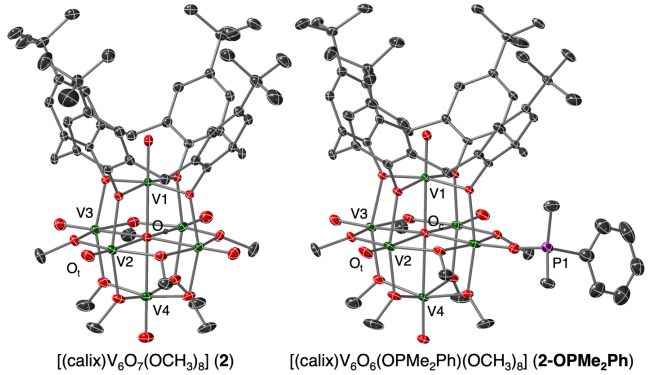

[(calix)$V_6O_7(OCH_3)_8$] (**2**) [(calix)$V_6O_6(OPMe_2Ph)(OCH_3)_8$] (**2-OPMe$_2$Ph**)

Figure 2. Molecular structures of **2** and **2-OPMe$_2$Ph** shown with 30% probability ellipsoids. Hydrogen atoms and solvent molecules have been removed for clarity. Key: V, dark green; O, red; C, grey; P, dark purple.

Activation of a vanadyl moiety positioned cis to the site-differentiated metal centre of the Lindqvist assembly is surprising, given the fact that BVS calculations of the parent cluster, **2**, reveal the pentavalent vanadium centre is located *trans* to the calix-ligated vanadyl moiety. Previous work from our research group has concluded that the formation of surface O-atom defects in the POV-alkoxide systems requires the presence of V^{V}=O moieties within the oxygenated parent cluster. A combination of electronic and structural factors can be invoked to rationalize the preferential OAT from an equatorial V=O moiety. First, the electron-withdrawing properties of the calix, bridging-phenoxide moieties that are positioned adjacent to the equatorial V=O bonds increase the electrophilicity of the terminal oxo moiety. These ligands stabilize the reduced V^{III} moiety generated following OAT. Furthermore, from a structural perspective, the formation of an oxygen-deficient V^{III} upon OAT in POV-alkoxides has been shown to result in a truncated bond distance between the V^{III} and the central oxo (2.0666(17)-2.120(5)).[13] In the case of a Lindqvist assembly bearing multiple defects, this structural perturbation dictates that the second OAT event must occur *cis* to the initial V^{III} site, giving rise to the formation of a much more stable $[V_2O_2]$ unit with a "square" geometry. In the fully-oxygenated, calix-functionalized POV-alkoxide cluster, the site-differentiated vanadyl moiety has a short V1-O_c bond length (2.1282(17) Å) when compared to other V-O_c lengths of the assembly (2.2848(17) – 2.3496(3) Å). This truncated V1-O_c bond length similarly directs formation of the V^{III}-$OPMe_2Ph$ unit in the position *cis* to the calix-protected V1 centre.

Comparing the reaction conditions required to form **2-OPMe$_2$Ph** (1 hour at 21° C), and those invoked previously for the isolation of the phosphine bound cluster $[V_6O_6(OMe)_{12}OPMe_2Ph]$ (7 hours at 70° C; Figure S6), it is evident that addition of the calix ligand induces a significant increase in the rate of OAT at the cluster surface. However, an explanation for this observation is not immediately apparent, given the analogous oxidation state distributions of vanadium centres in both assemblies. As such we turned to kinetic analysis to develop a thorough understanding of OAT in both **2** and $[V_6O_7(OMe)_{12}]$.

Initial experiments focused on establishing the rate expression for the transfer of an O-atom between **2** and PMe_2Ph. Pseudo-first order reaction conditions were used to measure changes in the rate of reaction as the concentration of each reactant is varied. By monitoring the consumption of the starting cluster through ^{1}H NMR spectroscopy, the order of each reactant is assigned as one, as shown in the rate expression found in Eqn 1 (Figures S7-S9, Tables S5-S6; see supporting information for experimental details):

$$-[\mathbf{2}]/dt = k[\mathbf{2}]^1[PMe_2Ph]^1 \qquad \text{Eqn 1}$$

From this rate expression, we are able to determine that the rate limiting step of OAT contains a one-to-one ratio of cluster and phosphine. Similar rate expressions have been observed in previous work analysing OAT at high-valent, mononuclear metal oxo complexes.[21, 22]

Similar experiments were performed to elucidate the rate expression describing OAT between PMe_2Ph and $[V_6O_7(OMe)_{12}]$. Results confirm an analogous rate expression, with reactants possessing an order of 1 (Eqn 2; Figures S10-S12, Tables S7-S8).

$$-[V_6O_7(OMe)_{12}]/dt = k[V_6O_7(OMe)_{12}]^1[PMe_2Ph]^1 \qquad \text{Eqn 2}$$

At first glance, the similarity of the two rate expressions suggests that both **2** and $[V_6O_7(OMe)_{12}]$ might perform OAT via analogous mechanisms. To more deeply probe differences in OAT in these two systems, we turned to Eyring analyses. Through this method, we are able to establish the activation parameters required for OAT to occur (Table 1, Figures S13-S16). The overall sign and magnitude of both the activation enthalpy and entropy values support the theory of a bimolecular rate-limiting reaction between the cluster and PMe_2Ph, however, the large difference in the activation parameters between the two clusters suggests a divergence of the OAT mechanism (Figure 3).

Table 1. Activation parameters for OAT between the respective cluster and PMe_2Ph. $\Delta G^{\ddagger}$ values are reported at 25° C.

Cluster	$\Delta H^{\ddagger}$ (kcal mol^{-1})	$\Delta S^{\ddagger}$ (cal mol^{-1} K^{-1})	$\Delta G^{\ddagger}$ (kcal mol^{-1})
2	17.8 ± 2.6	-10.4 ± 8.3	20.7 ± 4.9
$[V_6O_7(OMe)_{12}]$	12.2 ± 2.5	-55.9 ± 1.1	28.8 ± 2.2

The large entropic value associated with the transition state of OAT at $[V_6O_7(OMe)_{12}]$ dominates the overall free energy of activation and suggests a well-ordered intermediate is formed at the rate limiting step. This is consistent with a single OAT step for the reaction between $[V_6O_7(OMe)_{12}]$ and PMe_2Ph.[22] This

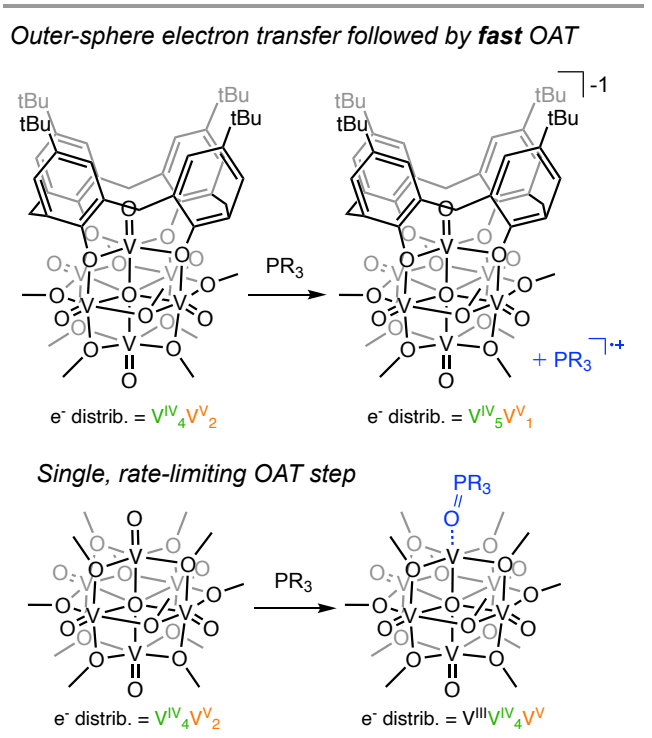

Figure 3. Disparate rate limiting steps in the proposed mechanisms of OAT in POV-alkoxide clusters.

contrasts with the much smaller magnitude of $\Delta S^{\ddagger}$ associated with OAT at **2**, in which the entropic term contributes little to the overall free energy of activation. Small $\Delta S^{\ddagger}$ values have been observed for OAT at metal oxide systems previously, and credited to the operativity of two possible mechanisms; the first being a rate-limiting, outer-sphere electron transfer from the phosphine to the cluster, while the second mechanism relies on the preformation of a precursor complex consisting of the cluster and phosphine, which then progresses through the transition state together.[21-28]

From the current data, we believe that a rate limiting step involving outer sphere electron transfer is the most likely pathway for the reaction of OAT at **2**. Previous studies into the electronic structure of the calix functionalized cluster reveal that incorporation of this ligand results in a positive shift in reduction potential for the assembly ($E_{1/2}$ (**2**) = -0.27 V vs. $Fc^{+/0}$), relative to that of $[V_6O_7(OMe)_{12}]$ ($E_{1/2}$ = -0.45 V vs. $Fc^{+/0}$).[16] This indicates that the reduction of **2** is more energetically favourable. An initial, rate-limiting step of electron transfer additionally supports the location of defect formation, despite the fact that the V^V sites are positioned trans to one another in the starting material, **2**. Given that electron transfer results in the reduction of the vanadyl group positioned *trans* from the calix-bound ion,[16] all sterically accessible vanadyl ions composing the Lindqvist core now occupy the 4+ oxidation state. As such, OAT to the phosphane occurs from a V=O moiety positioned *cis* to the site differentiated metal centre, resulting in the most state geometry of the $[V_2O_2]$ moiety (*vide supra*).

Here, we demonstrate the impact on kinetics of OAT through heteroleptic ligand substitution at the surface of POV-alkoxide clusters. Addition of a calix ligand induces a substantial increase in the rate of OAT relative to the unfunctionalized cluster, suggesting the ligand substitution pattern plays an integral role in the transfer of an O-atom. Kinetic analysis reveals significant differences in the activation energy for OAT from these assemblies, suggesting a divergence in the mechanisms of OAT. Functionalization of the cluster results in a preference toward a mechanism that is limited in rate by an outer sphere electron transfer, as opposed to the unfunctionalized cluster in which transfer of the oxygen atom controls the rate of reaction. Future work from our lab aims to explore disparate electronic structures of POV-alkoxide cluster and how these modifications impact OAT.

This research was funded by the National Science Foundation (CHE-1653195). E.M.M. is also the recipient of a Cottrell Scholar Award from Research Corporation for Science Advancement. The authors would like to acknowledge Dr. Sourav Chakraborty for helpful discussions regarding kinetic analysis of OAT.

Conflicts of interest

There are no conflicts to declare.

Notes and references

1 E. W. McFarland and H. Metiu, *Chem. Rev.*, 2013, **113**, 4391-4427.
2 J. C. Védrine, *Catalysts*, 2017, **7**.
3 P. Mars and D. W. van Krevelen, *Chem. Eng. Sci.*, 1954, **3**, 41-59.
4 W. Huang, *Acc.. Chem. Res.*, 2016, **49**, 520-527.
5 M. A. White, J. A. Johnson, J. T. Koberstein and N. J. Turro, *J. Am. Chem. Soc.*, 2006, **128**, 11356-11357.
6 B. E. Petel and E. M. Matson, *Chem. Commun.*, 2020, **56**, 13477-13490.
7 N. I. Gumerova and A. Rompel, *Nat. Rev. Chemistry*, 2018, **2**, 0112.
8 X. López, J. J. Carbó, C. Bo and J. M. Poblet, *Chem. Soc. Rev.*, 2012, **41**, 7537-7571.
9 B. E. Petel and E. M. Matson, *Inorg. Chem.*, 2021, **60**, 6855-6864.
10 B. E. Petel, R. L. Meyer, M. L. Maiola, W. W. Brennessel, A. M. Müller and E. M. Matson, *J. Am. Chem. Soc.*, 2020, **142**, 1049-1056.
11 S. Chakraborty, E. Schreiber, K. R. Sanchez-Lievanos, M. Tariq, W. W. Brennessel, K. E. Knowles and E. M. Matson, *Chemical Science*, 2021, **12**, 12744-12753.
12 E. Schreiber, B. E. Petel and E. M. Matson, *J. Am. Chem. Soc.*, 2020, **142**, 9915-9919.
13 B. E. Petel, W. W. Brennessel and E. M. Matson, *J. Am. Chem. Soc.*, 2018, **140**, 8424-8428.
14 A. A. Fertig, W. W. Brennessel, J. R. McKone and E. M. Matson, *J. Am. Chem. Soc.*, 2021, **143**, 15756-15768.
15 B. E. Petel, R. L. Meyer, W. W. Brennessel and E. M. Matson, *Chem. Sci.*, 2019, **10**, 8035-8045.
16 R. L. Meyer, P. Miró, W. W. Brennessel and E. M. Matson, *Inorg. Chem.*, 2021, **60**, 13833-13843.
17 J. Spandl, C. Daniel, I. Brüdgam and H. Hartl, *Angew. Chem. Int. Ed.*, 2003, **42**, 1163-1166.
18 C. Aronica, G. Chastanet, E. Zueva, S. A. Borshch, J. M. Clemente-Juan and D. Luneau, *J. Am. Chem. Soc.*, 2008, **130**, 2365-2371.
19 L. E. VanGelder, A. M. Kosswattaarachchi, P. L. Forrestel, T. R. Cook and E. M. Matson, *Chem. Sci.*, 2018, **9**, 1692-1699.
20 C. Daniel and H. Hartl, *J. Am. Chem. Soc.*, 2005, **127**, 13978-13987.
21 Y.-M. Lee, S. Kim, K. Ohkubo, K.-H. Kim, W. Nam and S. Fukuzumi, *J. Am. Chem. Soc.*, 2019, **141**, 2614-2622.
22 P. Singh, E. Stewart-Jones, M. C. Denler and T. A. Jackson, *Dalton Trans.*, 2021, **50**, 3577-3585.
23 J. Chen, H. Yoon, Y.-M. Lee, M. S. Seo, R. Sarangi, S. Fukuzumi and W. Nam, *Chem. Sci.*, 2015, **6**, 3624-3632.
24 S. Fukuzumi, *Coord. Chem. Rev.*, 2013, **257**, 1564-1575.
25 R. A. Marcus, *Ann. Rev. Phys. Chem.*, 1964, **15**, 155-196.
26 B. B. Sarma, I. Efremenko and R. Neumann, *J. Am. Chem. Soc.*, 2015, **137**, 5916-5922.
27 I. Kawafune and G.-e. Matsubayashi, *Bull. Chem. Soc. Japan*, 1995, **68**, 838-842.
28 A. M. Khenkin and C. L. Hill, *J. Am. Chem. Soc.*, 1993, **115**, 8178-8186.